ARL4C is A Key Driver of Gastric Cancer: An Integrative Analysis of ARL Family Members

Ning Xie
Xi'an Jiaotong University
Yunfan Bai
University of Tokyo
Lu Qiao
Xi'an Jiaotong University
Yuru Bai
Xi'an Jiaotong University
Jian Wu
Fourth Military Medical University
Yan Li
Xi'an Jiaotong University
Mingzuo Jiang
Fourth Military Medical University
Bing Xu
Xi'an Jiaotong University
Zhen Ni
Fourth Military Medical University
Ting Yuan
Fourth Military Medical University
Yongquan Shi
Fourth Military Medical University
Feng Xu
Xi'an Jiaotong University
Jinhai Wang
Xi'an Jiaotong University
Na Liu
Xi'an Jiaotong University
Lei Dong (dong556@126.com)

Research

Keywords: ARL family, gastric cancer, clinical values, ARL4C, TGF-β1

Posted Date: June 18th, 2020

DOI: https://doi.org/10.21203/rs.3.rs-35982/v1

Abstract

Background: As small GTP-binding proteins, ARL family members (ARLs) have been proved to regulate the malignant phenotypes of several cancers. However, the exact role of ARLs in gastric cancer (GC) remains elusive.

Methods: The expression status, interactive relations, potential pathways and genetic variations of ARLs are analyzed by bioinformatics tools. Machine learning models and enrichment analysis are performed by R platform. The biological functions of ARL4C are demonstrated by *in vitro* and *in vivo* experiments. The nomogram is further constructed to validate the prognostic value of ARL4C for GC patients.

Results: ARLs are significantly dysregulated in GC and involved in various cancer-related pathways. Subsequently, machine learning models identify ARL4C as one of the two most significant diagnostic and prognostic indicators among ARLs for GC. Furthermore, ARL4C silencing remarkably reverses the epithelial-mesenchymal transition (EMT) and inhibits the growth and metastasis of GC cells both i*n vitro* and *in vivo*. Moreover, enrichment analysis indicates that TGF-β1 is highly correlated with ARL4C, while ARL4C-related genes are significantly enriched in the TGF-β1 signaling. Correspondingly, we demonstrate that TGF-β1 treatment dramatically increases ARL4C expression, and ARL4C knockdown reverses TGF-β1-induced EMT possibly by inhibiting the expression of Smads, downstream factors of TGF-β1. Meanwhile, the coexpression of ARL4C and TGF-β1 worsens the prognosis of GC patients both in Kaplan-Meier analysis and nomogram model.

Conclusion: Our work is of significance for comprehensively understanding the crucial role of ARLs in the carcinogenesis of GC and the specific mechanisms underlying the GC-promoting effects of TGF-β1. More importantly, we uncover the great promise of ARL4C-targeted therapy in improving the efficacy of TGF-β1 inhibitors for GC patients.

Background

Gastric cancer (GC) is one of the most common malignancies worldwide (1) and the second leading cause of cancer-related deaths in China (2). GC is generally diagnosed only at the advanced stages because early GC is commonly asymptomatic or mild, leading to unsatisfactory prognosis (3). Thus, it is critical to further discover the molecular mechanisms underlying the tumorigenesis and progression of GC, and to identify novel promising biomarkers with higher sensitivity and specificity for early detection and prognosis evaluation.

The ADP-ribosylation factor-like family members (ARLs), which belong to ADP-ribosylation factor (ARF) subfamily, have been identified as key regulators that control membrane traffic, organelle structure and cytoskeleton organization (4). Accumulating evidences suggest that the aberrant regulation of ARLs plays a critical role in tumorigenesis of several cancers (5, 6). For example, ARL2 overexpression inhibits the malignant phenotypes of glioma cells and predicts better clinical outcomes of glioma patients (7), while its downregulation can suppress the invasion and growth of cervical cancer cells (8). ARL8B is

essential for the 3D invasive growth of prostate cancer both *in vitro* and *in vivo* (9). ARL4A could interact with Robo1 to promote cell migration by activating Cdc42 (10). A recent study reveals that ARL13B can enhance the migration and invasion of breast cancer cells via controlling integrin-mediated signaling pathway (11). Moreover, ARL4C overexpression promotes the progression of glioblastoma (GBM) *in vitro* and *in vivo* and indicates the poor prognosis for patients with GBM (12). However, the clinical values and biological functions of ARLs in GC remain elusive.

In this study, we firstly comprehensively investigate the expression profiles, hallmark pathways, genetic alterations and clinical values of ARLs in GC. We find that ARL4C and ARL13B are the most important diagnostic and prognostic indicators among ARLs for GC by machine learning models. Further *in vitro* and *in vivo* experiments demonstrate that down-regulation of ARL4C dramatically inhibits tumorigenesis and metastasis of GC cells. More importantly, we discover that ARL4C is highly related to TGF-β1 signaling pathway and mediates the TGF-β1-induced EMT, which is further confirmed by our discovery that the coexpression of ARL4C and TGF-β1 predicts worse survival for GC patients than ARL4C or TGF-β1, respectively.

Methods

Online bioinformatics analyses

The differential expression between gastric cancer and adjacent normal tissues from TCGA and GTEx datasets was displayed by GEPIA (http://gepia.cancer-pku.cn/detail.php) online tool (13). The Oncomine database (http://www.oncomine.org) was utilized to analyze the mRNA expression levels of ARLs in digestive system cancer (14). Gene-gene network and functions of ARLs were evaluated by GeneMANIA online tool (http://www.genemania.org) (15). Genomic alterations of ARLs in GC available at the TCGA database (TCGA, Firehose Legacy) were assessed using the cBioPortal online tool (http://cbioportal.org) (16). DNA methylation status of ARL4C was analyzed using MEXPRESS (https://mexpress.be/) (17). Kaplan-Meier plotter database (http://kmplot.com/analysis/) was used to investigate the predictive effects of ARLs on the overall survival of GC patients (18). All the analyses were performed according to the guidelines of these databases.

Gene set variation analysis (GSVA)

GSVA, a functional enrichment software, was utilized to estimate the variation of pathway activity over a sample population in an unsupervised manner (19). Hallmark gene sets and Kyoto Encyclopedia of Genes and Genomes (KEGG) pathway sets of ARLs in GC were carried out by “ggplot2” R package based on GSVA software. $P < 0.05$ and FDR < 0.05 were set as the screening standard.

Logistic Regression model construction and validation

TCGA and GTEx datasets were obtained from UCSC database (https://genome.ucsc.edu) to perform the analysis of ARLs’ diagnostic values on GC patients. The patients were randomly separated into training

(75%) and validation cohorts (25%). Logistic Regression was carried out to identify the diagnostic biomarkers with statistical significance in the training cohort using the “glm” function in R platform. Moreover, we evaluated the ability of predicted diagnostic markers in differentiating the GC patients in validation cohort.

Least absolute shrinkage and selection operator (LASSO) Cox regression analysis

GSE15459 cohort (tumor, n=200) in the Gene Expression Omnibus (GEO) was utilized to perform the prognostic analyses of ARLs in GC patients (https://www.ncbi.nlm.nih.gov/geo/query/acc.cgi?acc=GSE34942). LASSO Cox regression analysis was performed using “glmnet” R package. Tuning parameter (λ) selection in the LASSO model used 10-fold cross-validation via minimum criteria. A λ value of **0.0379** was chosen (λ.min) according to 10-fold cross-validation.

Enrichment analysis

Pearson’s correlation coefficient exceeding 0.5 indicates a good correlation between ARL4C and its co-expressed genes. We employed the “clusterProfiler” R package for Gene Ontology (GO) and KEGG enrichment analysis of genes co-expressed with ARL4C.

Kaplan-Meier analysis

We conducted Kaplan-Meier analysis of the effects of TGF-β1 and ARL4C on the overall survival of GC patients by R platform.

Nomogram construction and validation

Nomogram was built based on a multivariate Cox analysis using the “rms” R package. The predictive performance of the nomogram was then validated by Decision curve analysis (DCA) and calibration curves.

Clinical samples

The GC tissue microarray (ST-1503) was purchased from Xi’an Alenabio. In addition, 12 paired samples of primary GC and adjacent normal tissues were obtained from patients who had undergone GC surgery at Xijing Hospital of Digestive Diseases. All samples were clinically and pathologically verified.

Cell culture and transfection

The human gastric carcinoma cell lines (AGS, MKN45) were obtained from ATCC (Manassas, VA, USA) and maintained in DMEM medium supplemented with 10% fetal bovine serum and 1% penicillin-streptomycin solution. All cell lines were cultured at 37 °C in a humidified atmosphere containing 5% CO_2. The human shARL4C (NM_001282431) lentivirus was designed and constructed by GeneChem (Shanghai, China). siRNAs against human ARL4C were designed and constructed by GenePharma (Shanghai, China). The protocol was reported in a previous study (20).

Immunohistochemistry (IHC) and immunofluorescence (IF)

IHC was performed following the protocol from a previous study (20), while IF staining was performed according to the published protocol (21).

Western blot analysis

The protocol was reported in a previous study (20). The primary antibodies used in this study included anti-E-cadherin, anti-N-cadherin, anti-beta-catenin and anti-Vimentin (Cell Signal Technology (CST), USA), anti-GAPDH (10494-1-AP, Proteintech Technology, UK), and anti-ARL4C (ab122025, Abcam, USA).

In vitro and in vivo assays

We performed cell proliferation, colony formation assay, 3D invasion assay and xenografts assay following the protocols in a previous study (20).

Statistical analysis

Student's paired t-test was used to determine statistical significance of differences between two groups. Each experiment was carried out at least three times. Statistical analyses were conducted using SPSS software (Version 21.0). Images were obtained using GraphPad Prism software (Version 7.0). The counting data were represented by frequency or percentage, and the measurement data were expressed as the mean ± standard deviation (SD). $P < 0.05$ was considered statistically significant.

Results

The expression profiles and potential signaling pathways of ARLs in GC

As shown in Figure 1a, we firstly investigate the expression differences of ARLs between GC tissues and adjacent normal tissues using TCGA, GTEx and Oncomine databases (Figure 1b). We find that six ARLs (*i.e.*, ARL4C, ARL5A, ARL5B, ARL8A, ARL8B, ARL13B) are obviously up-regulated in GC tissues compared to adjacent normal tissues in TCGA and GTEx datasets ($P<0.01$). Meanwhile, 6 ARLs (*i.e.*, ARL2, ARL4C, ARL10, ARL11, ARL13B and ARL14) are aberrantly regulated in GC patients based on Oncomine (Figure S1a). Both in TCGA and Oncomine databases, ARL4C and ARL13B are significantly upregulated (Figure S1b).

Since small GTPase proteins commonly work synergistically as function hubs to regulate cell biological functions [21, 22], we conduct network analysis of ARLs at the gene level using the GeneMANIA tool, and find a large number of shared protein domains among ARLs (Figure 1c).

we further perform the correlation analysis of ARLs in GC using TCGA database. As shown in Figure 1d and Table S1: significant correlations are discovered among these genes. To explore the potential oncogenic pathways which ARLs are involved in, we analyze the correlation between the expression levels of ARLs and the activity of hallmark-related pathways using GSVA. As shown in Figure 1e and 1f,

various hallmark pathways of cancer are significantly associated with the expression of ARLs, including CHOLESTEROL HOMEOSTASIS (7/22), MYOGENESIS (5/22), UV RESPONSE UP (5/22), P53_PATHWAY (5/22). Meanwhile, the expression levels of ARL10 (n = 22), ARL13A (n = 12), ARL5B (n = 10), ARL15 (n = 8), and ARL4C (n = 8) are correlated with a higher number of pathways (Table S2).

Genetic alteration analysis of ARLs in GC

To comprehensively understand the expression profiles of ARLs in GC, we analyze the genetic alteration of ARLs in GC. The chromosome status (GRCh38/hg38) showed in Figure 2a and Table S3 clearly displays the genomic locations of 22 ARLs, and we find ARLs are unevenly distributed on different chromosomes. Furthermore, we conduct the exact genetic analysis using cBioPortal for Cancer Genomic. From the changes in protein structure of ARLs (mutation sites≥3), we find that ARL13B has more mutation sites than others (Figure 2b). Moreover, we discover varying degrees of genetic variation among the 22 ARLs (1.7% to 10.0%), and the mutation ratios of ARL4A, ARL13B and ARL16 are relatively higher, up to 10.0% (Figure S2a). We further check the alteration frequency of ARLs (mutation ratio≥8%) in various GC types. As shown in Figure 2c, copy number amplification obviously contributes to the mRNA expression alteration of ARLs in different GC types. More interestingly, DNA methylation analysis demonstrates that there is a negative correlation between mRNA expression and DNA methylation for most ARLs (R≥0.3, P□0.05) (Figure 2d). A recent study showed that deregulation of ARL4C is due to hypomethylation in its 3'-UTR in lung squamous cell carcinoma (22). Therefore, we further investigate the specific methylation sites of ARL4C using MEXPRESS tool and find that DNA methylation status of cg24441922 and cg11509907 sites of the 3'-UTR is significantly negatively related to ARL4C mRNA expression (Figure S2b and Table S4). Taken together, these results suggest that DNA methylation is also involved in the epigenetic regulation of ARLs.

The diagnostic and prognostic values of ARLs for GC

We further assess the diagnostic and prognostic values of ARLs in GC patients based on the TCGA, GTEx and GEO datasets. Firstly, we construct the Logistic Regression model to test the usefulness of ARLs in GC diagnosis. All samples are randomly separated into training (75%) and validation (25%) cohorts. All ARLs in the training cohort are identified and featured with nonzero coefficients by Logistic regression model. Then, diagnostic markers with high significance are selected using stepwise method ("both" method). As shown in Figure 3a, we identify nine ARLs as the potential diagnostic markers for GC. Moreover, we evaluate the ability of predicted diagnostic markers in differentiating the GC patients from the normal in validation cohort. The result suggest that our selected diagnostic markers have a high accuracy of prediction (Area Under Curve (AUC) = 0.929) (Figure S3a).

Furthermore, we analyze the effects of ARLs on the overall survival (OS) of GC patients using the Kaplan-Meier (K-M) plotter. We observe that 9 ARLs (*i.e.*, ARL1, ARL4C, ARL5A, ARL5B, ARL9, ARL13B, ARL15, ARL17A and ARL17B) are significantly related to patient prognosis (Figure S3b). Thus, ARLs are of great significance for assessing prognosis for GC patients. Then, we further identify the key prognostic markers for the purpose of avoiding overfitting of the predictive model with the minimum criteria s via conducting

LASSO Cox regression model univariate and multivariate Cox regression models (Figure 3b and Figure S3c),where eight ARLs (ARL1, ARL4C, ARL5C, ARL6, ARL13B, ARL14, ARL15 and ARL16) are selected that are reliably associated with OS. The univariate and multivariate Cox regression models are also undertaken to study the prognostic values of all ARLs for GC (Figure 3c and 3d). As the Venn diagram integrated diagnostic analysis model and prognostic analysis models shown in Figure 3e, we acknowledge that ARL4C and ARL13B are the most important markers for diagnosis and prognosis for GC patients among all ARLs.

ARL13B has been previously reported to play a critical role in promoting proliferation, migration and invasion of GC cells and is associated with poor prognosis of GC patients (23). However, the biological functions of ARL4C in gastric tumorigenesis remain unclear. Therefore, we evaluate the protein expression level of ARL4C by IHC in a cohort of 142 GC patients (Cohort Ⅱ). Higher ARL4C expression is found in primary GC samples compared with normal gastric mucosa tissues (Figure 3f). Furthermore, we identify the ARL4C expression in frozen tumor and adjacent mucosa tissues of 12 GC patients at the Xijing Hospital of Digestive Diseases (Cohort Ⅰ) by Western blot analysis. The results indicate that the protein expression of ARL4C in the tumor tissues is significantly higher than that in the adjacent mucosa tissues (Figure 3g). Meanwhile, ARL4C overexpression could remarkably dampen the prognosis of GC patients after adjusting for several confounding factors, including subtype, Lauren classification, stage, age at surgery and gender (Figure S3d).

ARL4C knockdown decreases the proliferation and metastasis of GC cells *in vitro* and *in vivo* as well as reverses EMT

Given that ARL4C is involved in regulating the biological behaviors of various tumors, we examine whether ARL4C acts as an oncogene in GC cells *in vitro* and *in vivo*. In contrast to other small G proteins, ARL4C activity is regulated by its expression level rather than the switch between GDP- and GTP-bound status induced by regulators. Thus, we explore the role of ARL4C in the tumorigenesis of GC by constructing ARL4C knockdown GC cells. AGS and MKN45 cells are transfected with shRNA and siRNA against ARL4C. Multiple clones stably transfected with lentivirus are selected and confirmed by PCR and western blot analyses (Figure S4a and S4b). CCK-8 assays reveal that ARL4C downregulation significantly reduces cell growth compared with the control (Figure 4a), which is further confirmed by colony forming assays (Figure 4b). Furthermore, the *in vivo* analysis shows that silencing ARL4C in MKN45 cells causes obvious reductions in tumor weight and volume in nude mice (Figure 4c). The 3D invasion experiment, as shown in Figure 4d, indicates that ARL4C knockdown can decrease the invasion ability of GC cells in 3D culture. The *in vivo* metastatic assay also indicates that the downregulation of ARL4C decreases the incidence of lung metastasis and the number of metastatic lung nodules (Figure 4e). Overall, these results suggest that ARL4C may play a critical role in GC growth and metastasis both *in vitro* and *in vivo.*

Epithelial-mesenchymal transition (EMT) is involved in tumor aggressive progression. To confirm the role of ARL4C in regulating EMT of GC cells, we evaluate the expression changes of EMT markers after

ARL4C silencing. Western-blot and RT-PCR analyses shos that downregulation of ARL4C leads to the increased expression of E-cadherin and decreased expression of N-cadherin and Vimentin compared with the control group (Figure 5a and 5b). Furthermore, the IF assays show similar results (Figure 5c). Additionally, we investigate the correlation coefficients between ARL4C and EMT markers based on the TCGA data and find that ARL4C is positively related to Vimentin (Figure S5c).

ARL4C acts a mediator of TGF-β1/Smad signaling in GC

To uncover the underlying mechanisms of ARL4C in GC, we explore the TCGA database to identify the genes related to ARL4C. As shown in Figure S5a and S5b, we identify that numbers of GC-related genes are highly correlated with ARL4C, among which TGF-β1 is the most significant gene in GC (R=0.851, P 0.01). GO and KEGG enrichment analyses indicate that the ARL4C-associated genes (R≥0.5, P 0.05) are significantly involved in the cellular response to TGF-β stimulus and TGF-β signaling pathway (Figure 6a and 6b).

As TGF-β1 is identified as an important inducer of the malignant progression of cancer, we investigate whether ARL4C might participate in TGF-β1-induced progression of GC. We treat AGS and MKN45 cells with 10 ng/ml TGF-β1 for 24 and 48 h. Following TGF-β1 stimulation, compared with the control, ARL4C is significantly upregulated in AGS and MKN45 cells. In particular, TGF-β1-induced ARL4C expression is in a time-dependent manner in AGS cells (Figure 6c). In addition, Western blot analysis and immunofluorescence analysis show the downregulation of ARL4C decreases the expression levels of Smad3, phosphorylated-Smad2 (p-Smad2) and phosphorylated-Smad3 (p-Smad3) in the AGS and MKN45 cells (Figure 6d-6e and Figure S4c). Meanwhile, TCGA correlation analysis shows that ARL4C is positively related to Smad2 and Smad3 with high correlation coefficients (Figure S5c). These data suggest that ARL4C may mediate the TGF-β1/Smad signaling pathway. Besides, TGFβ-1-induced EMT is reversed when ARL4C is silenced in MKN45 cells (Figure 6f and 6g).

ARL4C enhances the TGF-β1-mediated poor prognosis of GC patients

To translate the above findings into clinical significance, we analyze clinical data of ARL4C and TGF-β1 expression in GC patients from GSE15459 cohort. We divide the samples into 4 groups according to the expression status of ARL4C and TGF-β1: group 1 ($ARL4C^{low}$/ $TGF\text{-}\beta1^{low}$), group 2 ($ARL4C^{high}$/ $TGF\text{-}\beta1^{low}$), group 3 ($ARL4C^{low}$/ $TGF\text{-}\beta1^{high}$) and group 4 ($ARL4C^{high}$/ $TGF\text{-}\beta1^{high}$). Kaplan-Meier analysis shows that elevated expression of TGF-β1 or ARL4C is associated with shorter OS of GC patients. Furthermore, patients with coexpression of TGF-β1 and ARL4C have the lowest OS (Figure 7a).

Next, we construct a predictive nomogram based on overall mortality (OM) via multivariate Cox regression model. The nomogram incorporates six variables: age, the expression status of TGF-β1 and ARL4C, gender, stage, molecular subtype and Lauren subtype. As shown in Figure 7b, to evaluate the individual's probability of overall mortality, values for the prognostic factors must be determined. Each independent prognostic factor is assigned an exact score scale, the points must be added up to obtain

the total risk score at 3, 5, and 8 years. The OM probability can be read from the X-axis (total risk score) to the predicted the corresponding probabilities of independent prognostic factors on the left Y-axis.

The nomogram demonstrates that stage of GC patients contributes significantly to the individual's probability of overall mortality and patients in stage □ have the highest mortality. Secondly, the expression status of TGF-β1 and ARL4C is a critical prognostic factor for GC patients. Group 4 ($ARL4C^{high}$/ $TGF\text{-}\beta1^{high}$) has the higher probability of OM than group 1 ($ARL4C^{low}$/ $TGF\text{-}\beta1^{low}$), group 2 ($ARL4C^{high}$/ $TGF\text{-}\beta1^{low}$) and group 3 ($ARL4C^{low}$/ $TGF\text{-}\beta1^{high}$) at 3, 5 and 8 years. We then adopt DCA to verify the prognostic accuracy of the nomogram in OS prediction. The results show that the best net benefit is similar with the prediction of the nomogram at 3, 5 and 8 years (Figure 7c and 7d).

The calibration curves of the nomogram at 3, 5 and 8 years are very close to the best prediction curve, showing a great consistency between the predicted OS rates and the actual observations (Figure 7e). Taken together, these results suggest that ARL4C is critical for TGF-β1-mediated poor clinical outcomes for GC patients.

Discussion

ARLs have been reported to play important roles in cancer progression. Nevertheless, the exact role of ARLs in GC and the underlying molecular mechanisms are not well illustrated. The present study aims to comprehensively understand the expression patterns, correlation, genetic alteration, diagnostic values, prognostic values and potential functions of ARLs in GC by integrated bioinformatics analysis and experiments.

The expression profiles of ARLs are firstly explored using TCGA, GTEx and Oncomine databases, which demonstrate that ARLs are commonly dysregulated in GC. Accumulating evidences suggest that the cross-talk and collaboration between small GTPase proteins are causatively involved in several cellular processes and diseases (24–27). In this study, co-expression and correlation analyses demonstrate that the expression levels of ARLs in GC show high correlations. Meanwhile, there are majorities of shared protein domains among ARLs. Furthermore, according to the Hallmark gene sets analysis, we discover that ARLs may modulate numbers of cancer-related pathways, and more interestingly, several ARLs are involved in the same pathways. For instance, ARL5C, ARL10, ARL13B and ARL13A are enriched in P53-PATHWAY which is critical to GC progression (28). Taken together, our bioinformatics analysis indicates that dysregulated ARLs might function synergistically to modulate various signaling pathways in GC.

Our further genetic analysis indicates that the genetic alterations, including copy number alteration and DNA methylation status, are involved in the misregulation of ARLs in GC. Particularly, we find that DNA methylation status is inversely correlated with the mRNA expression of several ARLs in GC. It is generally accepted that DNA methylation is a major epigenetic process that plays a critical role in different stages of cancer evolution and development (29). Fujii's study showed that the hypomethylation in the 3'-UTR induces the overexpression of ARL4C in lung cancer which contributes to the malignant phenotypes of

cancer cells (22). In line with this, we find that the methylation status at cg24441922 site is significantly negatively related to ARL4C mRNA expression in GC. Overall, we acknowledge that DNA methylation status might be involved in the dysregulation and oncogenic functions of ARLs in GC.

Multiple machine learning models are constructed to evaluate the diagnostic and prognostic values of ARLs in GC. After comprehensively analyzing the logistic regression model, univariate Cox regression model, multivariate Cox regression model and LASSO Cox regression model, we firstly reveal that ARL4C and ARL13B are the most critical indicators for diagnosis and prognosis in GC among all ARLs. Consistent with our results, recent studies have uncovered that overexpression of ARL13B and ARL4C is correlated strongly with the poor prognosis of GC patients (23, 30). ARL13B may worsen the survival and stimulate GC cell proliferation and migration both *in vitro* and *in vivo*. Meanwhile, it might regulate Smo trafficking and activate the Hedgehog signaling pathway (23). On the other hand, *in vitro* assays suggest that ARL4C-knockdown would inhibit the migration capacity of GC cells under 2D culture and reduce protein expression of Slug which is related to EMT [20]. However, a previous study has shown the oncogenic function of ARL4C exhibits dramatic differences between *in vitro* and *in vivo* assays in colon cancer as well as lung cancer (21). Therefore, we perform 3D and *in vivo* experiments to further assess the effects of ARL4C on the growth and metastasis of GC cells. Our results solidly support a close association between ARL4C expression and GC malignant phenotypes. Downregulation of ARL4C could obviously inhibit cell proliferation and metastasis both *in vitro* and *in vivo*, while ARL4C knockdown has significant effects on EMT, as indicated by the increased expression of epithelial marker (E-cadherin) and decreased expression of mesenchymal markers (N-cadherin and vimentin).

TGF-β1, as a pleiotropic cytokine, orchestrates complicated signals to modulate tumorigenesis and promote cancer progression (31). Increasing preclinical and clinical studies have identified TGF-β signaling as a determinant in immunotherapy (32). TCGA datamining in our study indicates TGF-β1 as the most significant ARL4C-related gene in GC. Further functional enrichment analysis also demonstrates that the ARL4C-associated genes in GC are significantly linked to the TGF-β-related signaling. Thus, we speculate that ARL4C could participate in TGF-β1 pathway. Accordingly, the expression of ARL4C is obviously upregulated with the stimulation of TGF-β1 in GC cells, while knockdown of ARL4C weakens p-Smad2/3 expression levels and impairs TGF-β1-induced EMT. These results indicate that ARL4C may act as a mediator between TGF-β1 and Smads in GC. Remarkably, Kaplan-Meier analysis shows that ARL4C (+)/TGF-β1 (+) co-expression is associated with shorter OS of GC patients. To perform prognostic prediction more precisely, we further construct an OS nomogram based on the expression status of ARL4C and TGF-β1 as well as other clinical variables. Consistently, our nomogram indicates that the ARL4C (+)/TGF-β1 (+) group is an independent risk factor and shows the highest mortality at 3, 5 and 8 years. In sum, ARL4C may act a mediator of TGF-β1/Smad signaling and enhance the TGF-β1-mediated poor prognosis in GC. Our results demonstrate the great promise of ARL4C targeting treatment in improving the effectiveness of TGF-β1 inhibitors for GC patients.

Conclusion

To our knowledge, it is for the first time that the expression patterns, genetic alterations, signaling pathways, diagnostic values and prognostic values of ARLs in GC have been fully explored. Our results identify ARL4C as one of the two most significant diagnostic and prognostic indicators in GC. ARL4C would function as an oncogene in gastric tumorigenesis by promoting cell proliferation, metastasis and EMT. Furthermore, ARL4C could function as a mediator of TGF-β1 signaling and enhance TGF-β1-associated poor prognosis in GC (Fig. 8). Our studies provide an overall insight into the specific roles of ARLs that benefits the development of novel strategies for GC detection and treatment.

Abbreviations

ARLs: ADP-ribosylation factor-like family members; GC: gastric cancer; EMT: epithelial-mesenchymal transition; GSVA: gene set variation analysis; LASSO: least absolute shrinkage and selection operator; GEO: gene expression omnibus; KEGG: kyoto encyclopedia of genes and genomes; GO: gene ontology; DCA: decision curve analysis; AUC: area under curve; OS: overall survival; OM: overall mortality.

Declarations

Acknowledgements

We sincerely appreciate all co-authors.

Contribution of co-authors

Ning Xie performed the majority of experimental work as well as data analysis and authored the manuscript. Yunfan Bai and Lu Qiao contributed equally to this work. Yuru Bai assisted with immunohistochemistry and all cell experiments. Jian Wu assisted in authoring the manuscript. Yan Li assisted with CCK-8 and data analysis. Mingzuo Jiang and Bing Xu assisted with 3D-invasion assay and RT-PCR. Zhen Ni and Ting Yuan assisted in some animal experiments. Feng Xu and Yongquan Shi assisted in authoring the manuscript. Jinhai Wang provided funding. Na Liu provided funding and assisted in authoring the manuscript. Lei Dong provided funding, coordinated the project and participated in authoring the manuscript. All authors reviewed the results and approved the final version of the manuscript.

Funding

The study is supported by grants from the National Natural Science Foundation of China (No. 81872397) and the State Key Laboratory of Cancer Biology (No. CBSKL201730).

Availability of data and materials

Not applicable.

Ethics approval and consent to participate

Ethics Committee Approval and Patient Consent: this study was approved by Xijing Hospital's Protection of Human Subjects Committee. Informed consent was obtained from each patient.

Conflicts of interest

The authors declare no conflict of interests.

Consent for publication

Authors confirmed that this work can be published. The content of this manuscript is original and it has not yet been accepted or published elsewhere.

Author details

[a] Department of Gastroenterology, the Second Affiliated Hospital of Xi'an Jiaotong University, Shaanxi, China;

[b] Shaanxi Key Laboratory of Gastrointestinal Motility Disorders, Xi'an Jiaotong University, Shaanxi, China;

[c] Department of Computational Biology and Medical Sciences, Graduate School of Frontier Sciences, University of Tokyo, Kashiwa, Japan;

[d] State Key Laboratory of Cancer Biology, National Clinical Research Center for Digestive Diseases and Xijing Hospital of Digestive Diseases, the Fourth Military Medical University, Xi'an, Shaanxi, China;

[e] The Key Laboratory of Biomedical Information Engineering of Ministry of Education, School of Life Science and Technology, Xi'an Jiaotong University, Xi'an, Shaanxi 710049, China;

[f] Bioinspired Engineering and Biomechanics Center (BEBC), Xi'an Jiaotong University, Xi'an, Shaanxi 710049, China.

References

1. RL S, KD M, Cancer statistics AJ. 2019. CA: a cancer journal for clinicians. 2019;69(1):7–34.
2. W C, R Z, PD B, S Z, H Z, F B, et al. Cancer statistics in China, 2015. CA: a cancer journal for clinicians. 2016;66(2):115–32.
3. BJ D, DL B, C C JR, AA M. J, SM H. Gastric adenocarcinoma: review and considerations for future directions. Annals of surgery. 2005;241(1):27–39.
4. JG D. CL J. ARF family G proteins and their regulators: roles in membrane transport, development and disease. Nature reviews Molecular cell biology. 2011;12(6):362–75.
5. Casalou C, Faustino A, Barral DC. Arf proteins in cancer cell migration. Small GTPases. 2016;7(4):270–82.

6. Burd CG, Strochlic TI, Setty SR. Arf-like GTPases: not so Arf-like after all. Trends in cell biology. 2004;14(12):687–94.
7. Wang Y, Guan G, Cheng W, Jiang Y, Shan F, Wu A, et al. ARL2 overexpression inhibits glioma proliferation and tumorigenicity via down-regulating AXL. BMC Cancer. 2018;18(1):599.
8. Peng R, Men J, Ma R, Wang Q, Wang Y, Sun Y, et al. miR-214 down-regulates ARL2 and suppresses growth and invasion of cervical cancer cells. Biochem Biophys Res Commun. 2017;484(3):623–30.
9. SS D, AL G, DT C, JL MSCAS. C, et al. The Arf-like GTPase Arl8b is essential for three-dimensional invasive growth of prostate cancer in vitro and xenograft formation and growth in vivo. Oncotarget. 2016;7(21):31037–52.
10. Chiang TS, Lin MC, Tsai MC, Chen CH, Jang LT, Lee FS. ADP-ribosylation factor-like 4A interacts with Robo1 to promote cell migration by regulating Cdc42 activation. Molecular biology of the cell. 2019;30(1):69–81.
11. Casalou C, Faustino A, Silva F, Ferreira IC, Vaqueirinho D, Ferreira A, et al. Arl13b Regulates Breast Cancer Cell Migration and Invasion by Controlling Integrin-Mediated Signaling. Cancers. 2019;11(10).
12. Chen Q, Weng HY, Tang XP, Lin Y, Yuan Y, Li Q, et al. ARL4C stabilized by AKT/mTOR pathway promotes the invasion of PTEN-deficient primary human glioblastoma. J Pathol. 2019;247(2):266–78.
13. Tang Z, Li C, Kang B, Gao G, Li C, Zhang Z. GEPIA: a web server for cancer and normal gene expression profiling and interactive analyses. Nucleic acids research. 2017;45(W1):W98-w102.
14. Rhodes DR, Kalyana-Sundaram S, Mahavisno V, Varambally R, Yu J, Briggs BB, et al. Oncomine 3.0: genes, pathways, and networks in a collection of 18,000 cancer gene expression profiles. Neoplasia (New York NY). 2007;9(2):166–80.
15. Warde-Farley D, Donaldson SL, Comes O, Zuberi K, Badrawi R, Chao P, et al. The GeneMANIA prediction server: biological network integration for gene prioritization and predicting gene function. Nucleic acids research. 2010;38(suppl_2):W214-W20.
16. Gao J, Aksoy BA, Dogrusoz U, Dresdner G, Gross B, Sumer SO, et al. Integrative analysis of complex cancer genomics and clinical profiles using the cBioPortal. Sci Signal. 2013;6(269):pl1.
17. Koch A, De Meyer T, Jeschke J, Van Criekinge W. MEXPRESS: visualizing expression, DNA methylation and clinical TCGA data. BMC Genomics. 2015;16:636.
18. Szasz AM, Lanczky A, Nagy A, Forster S, Hark K, Green JE, et al. Cross-validation of survival associated biomarkers in gastric cancer using transcriptomic data of 1,065 patients. Oncotarget. 2016;7(31):49322–33.
19. S H, R C, J G. GSVA: gene set variation analysis for microarray and RNA-seq data. BMC bioinformatics. 2013;14:7.
20. Jiang M, Wu N, Xu B, Chu Y, Li X, Su S, et al. Fatty acid-induced CD36 expression via O-GlcNAcylation drives gastric cancer metastasis. Theranostics. 2019;9(18):5359–73.

21. Fujii S, Matsumoto S, Nojima S, Morii E, Kikuchi A. Arl4c expression in colorectal and lung cancers promotes tumorigenesis and may represent a novel therapeutic target. Oncogene. 2015;34(37):4834–44.
22. Fujii S, Shinjo K, Matsumoto S, Harada T, Nojima S, Sato S, et al. Epigenetic upregulation of ARL4C, due to DNA hypomethylation in the 3'-untranslated region, promotes tumorigenesis of lung squamous cell carcinoma. Oncotarget. 2016;7(49):81571–87.
23. Shao J, Xu L, Chen L, Lu Q, Xie X, Shi W, et al. Arl13b Promotes Gastric Tumorigenesis by Regulating Smo Trafficking and Activation of the Hedgehog Signaling Pathway. Cancer research. 2017;77(15):4000–13.
24. Holmes WR, Edelstein-Keshet L. Analysis of a minimal Rho-GTPase circuit regulating cell shape. Physical biology. 2016;13(4):046001.
25. Margiotta A, Bucci C. Coordination between Rac1 and Rab Proteins: Functional Implications in Health and Disease. Cells. 2019;8(5).
26. Kjos I, Vestre K, Guadagno NA, Borg Distefano M, Progida C. Rab and Arf proteins at the crossroad between membrane transport and cytoskeleton dynamics. Biochimica et biophysica acta Molecular cell research. 2018;1865(10):1397–409.
27. C AM. P, O B, C B. Rab7a regulates cell migration through Rac1 and vimentin. Biochimica et biophysica acta Molecular cell research. 2017;1864(2):367–81.
28. ML AH. B, A J, G L. The multiple mechanisms that regulate p53 activity and cell fate. Nature reviews Molecular cell biology. 2019;20(4):199–210.
29. Ebrahimi V, Soleimanian A, Ebrahimi T, Azargun R, Yazdani P, Eyvazi S, et al. Epigenetic modifications in gastric cancer: Focus on DNA methylation. Gene. 2020;742:144577.
30. Hu Q, Masuda T, Sato K, Tobo T, Nambara S, Kidogami S, et al. Identification of ARL4C as a Peritoneal Dissemination-Associated Gene and Its Clinical Significance in Gastric Cancer. Ann Surg Oncol. 2018;25(3):745–53.
31. J M. TGFβ signalling in context. Nature reviews Molecular cell biology. 2012;13(10):616–30.
32. A T-R CN. R C, J C, S F, E R, et al. Targeting the TGFβ pathway for cancer therapy. Pharmacol Ther. 2015;147:22–31.

Figures

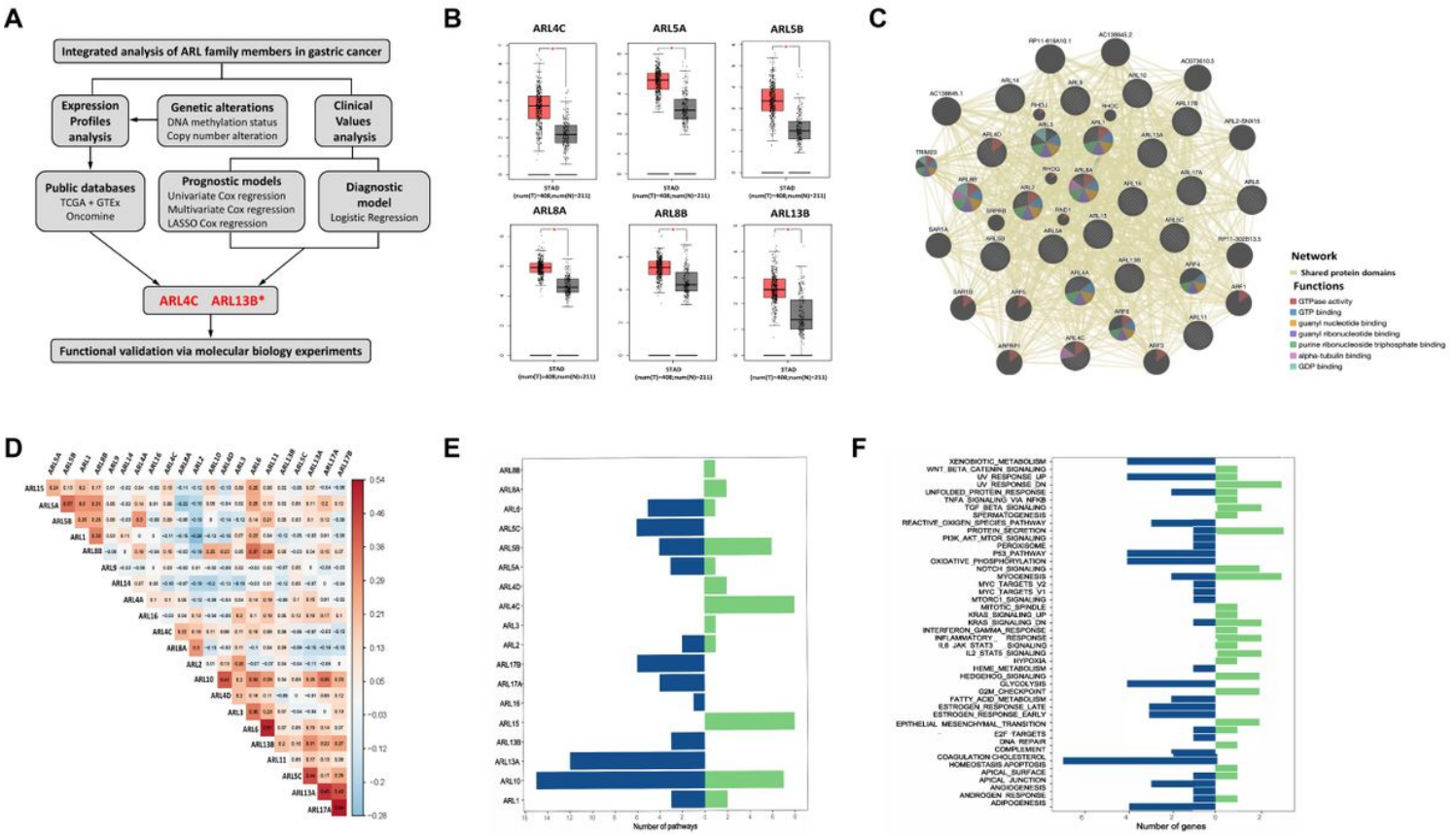

Figure 1

Expression profiles and pathway analysis of ARLs in GC. (a) Schematic diagram of research flow. (b) Box plots show the differential expression of ARLs (ARL4C, ARL5A, ARL5B, ARL8A, ARL8B and ARL13B) between GC (red) and adjacent normal tissues (grey) from TCGA by GEPIA (*P<0.01). (c) Gene–gene interaction network among ARLs. Each node represents a gene. The inter-node connection lines represent the network types and the node colors represent the possible functions of respective genes. (d) The heat map shows the Pearson's Correlation values among ARLs in TCGA dataset. (e) The bar diagram shows the number of pathways regulated by ARLs explored by GSVA. (f) The bar diagram displays the biological processes and signaling pathways regulated by the certain number of ARLs.

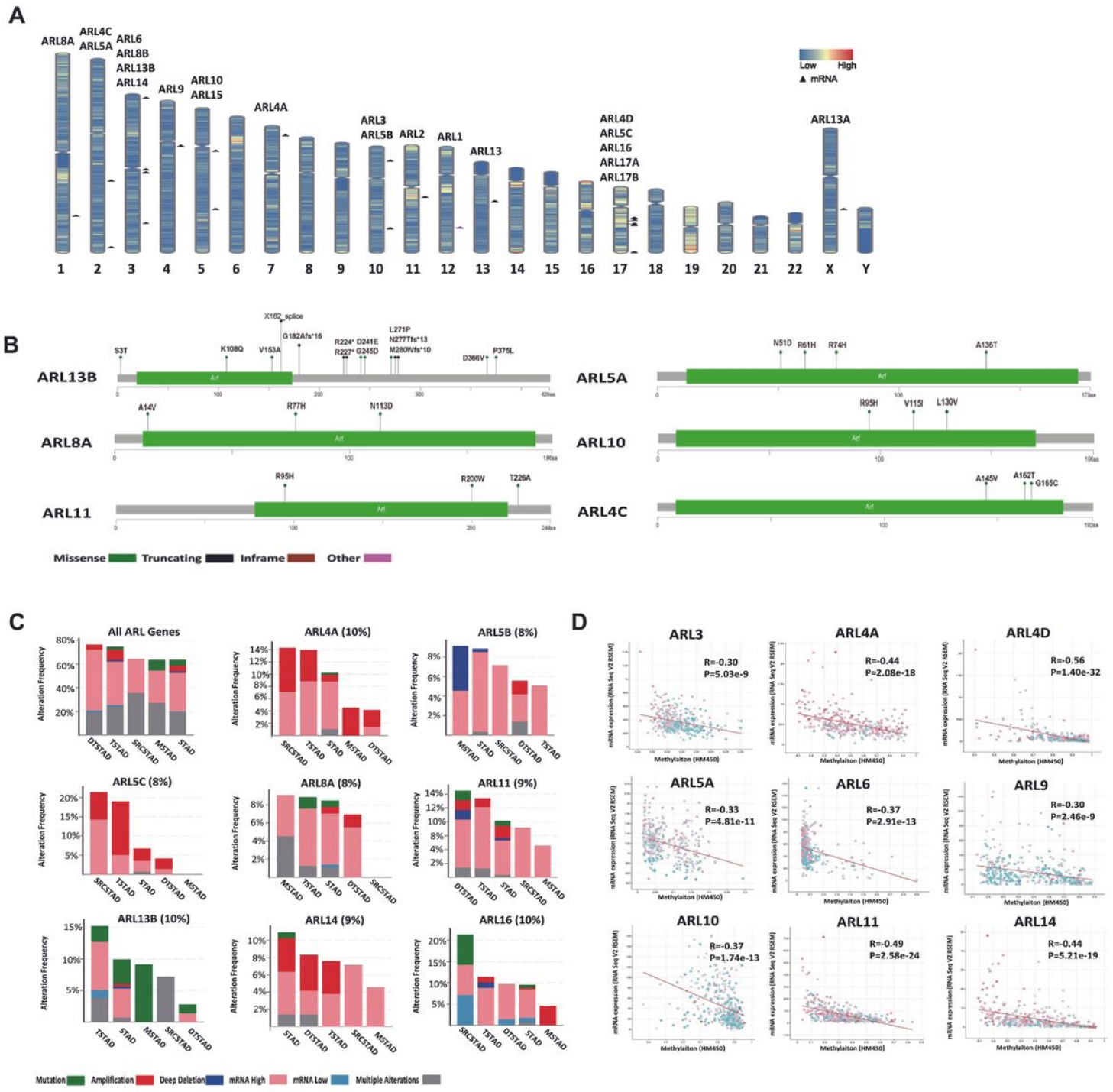

Figure 2

Genetic alterations of ARLs in GC. (a) The genomic locations for ARLs (GRCh38/hg38). (b) Mutation information of ARLs proteins in GC. (c) Alteration frequency of ARLs in different GC subtypes including mutations, amplification, deep deletion, mRNA dysregulation and multiple changes. SRCSTAD: Signet ring cell carcinoma of the stomach; TSTAD: Tubular stomach adenocarcinoma; STAD: Stomach adenocarcinoma; DTSTAD: Diffuse type stomach adenocarcinoma; MSTAD: Mucinous stomach adenocarcinoma. (d) Association of ARLs mRNA expression with DNA methylation.

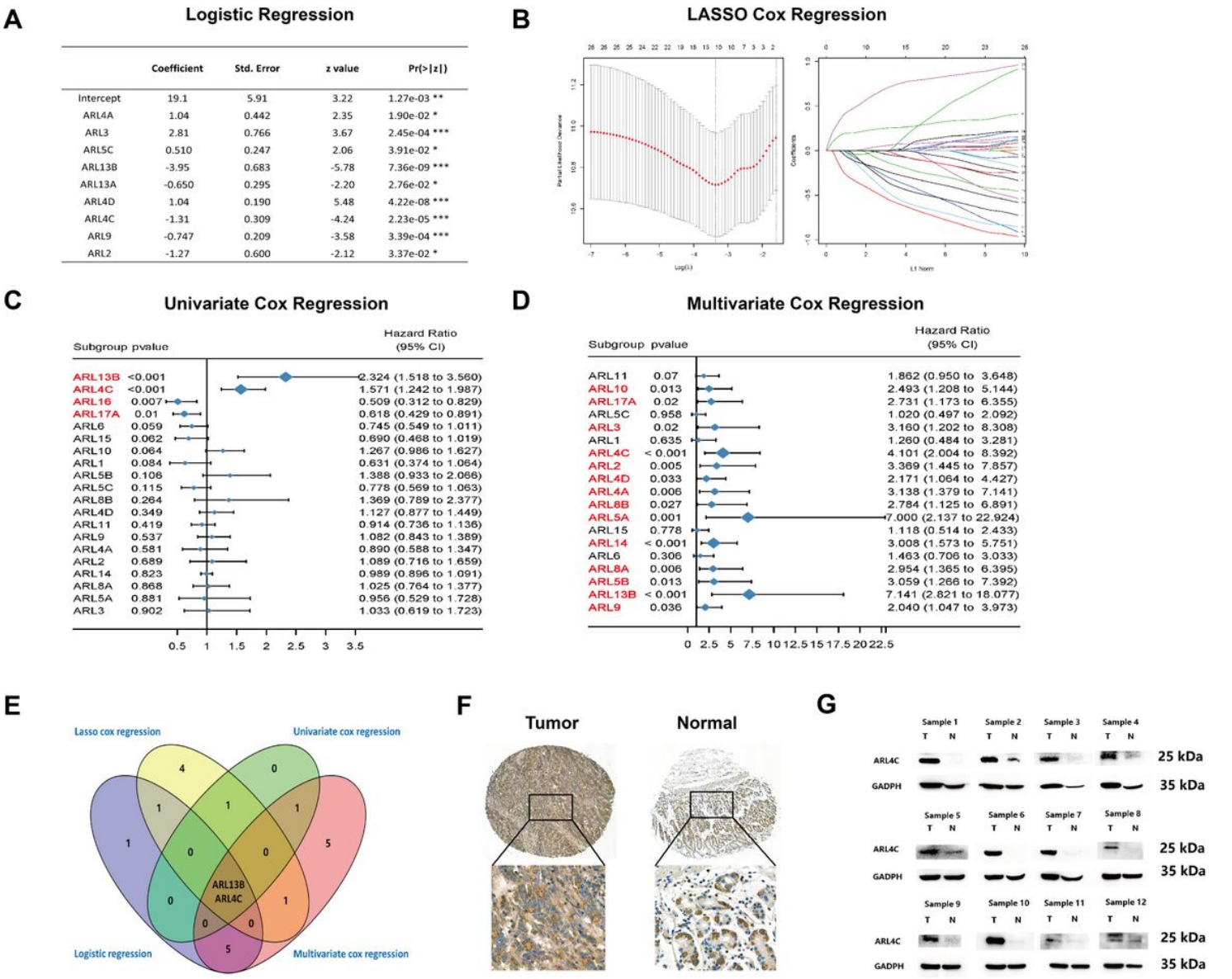

Figure 3

Analysis of the diagnostic and prognostic values of ARLs in GC. (a) Logistic Regression analysis of ARLs in GC. (b) LASSO coefficient profiles of the OS-related ARLs. A coefficient profile plot is produced against the log λ sequence. Vertical line is drawn at the value selected using 10-fold cross-validation, where optimal lambda results in 22 nonzero coefficients. (c) The forest plot shows the distribution of OS hazard ratios across ARLs in GC patients in univariate Cox model. (d) The forest plot shows the distribution of OS hazard ratios across ARLs in GC patients in multivariate Cox model. (e) The Venn diagram shows that four machine learning models jointly identify ARL13B and ARL4C as the most critical diagnostic and prognostic indicators for GC. (f) Representative images of IHC staining of ARL4C in GC and adjacent normal tissues. Scale bars represent 500 μm (low magnification) and 100 μm (high magnification). (g) Representative images of Western blot analysis of ARL4C expression in frozen tumor and adjacent mucosa tissues of 12 GC patients from Xijing Hospital of Digestive Diseases.

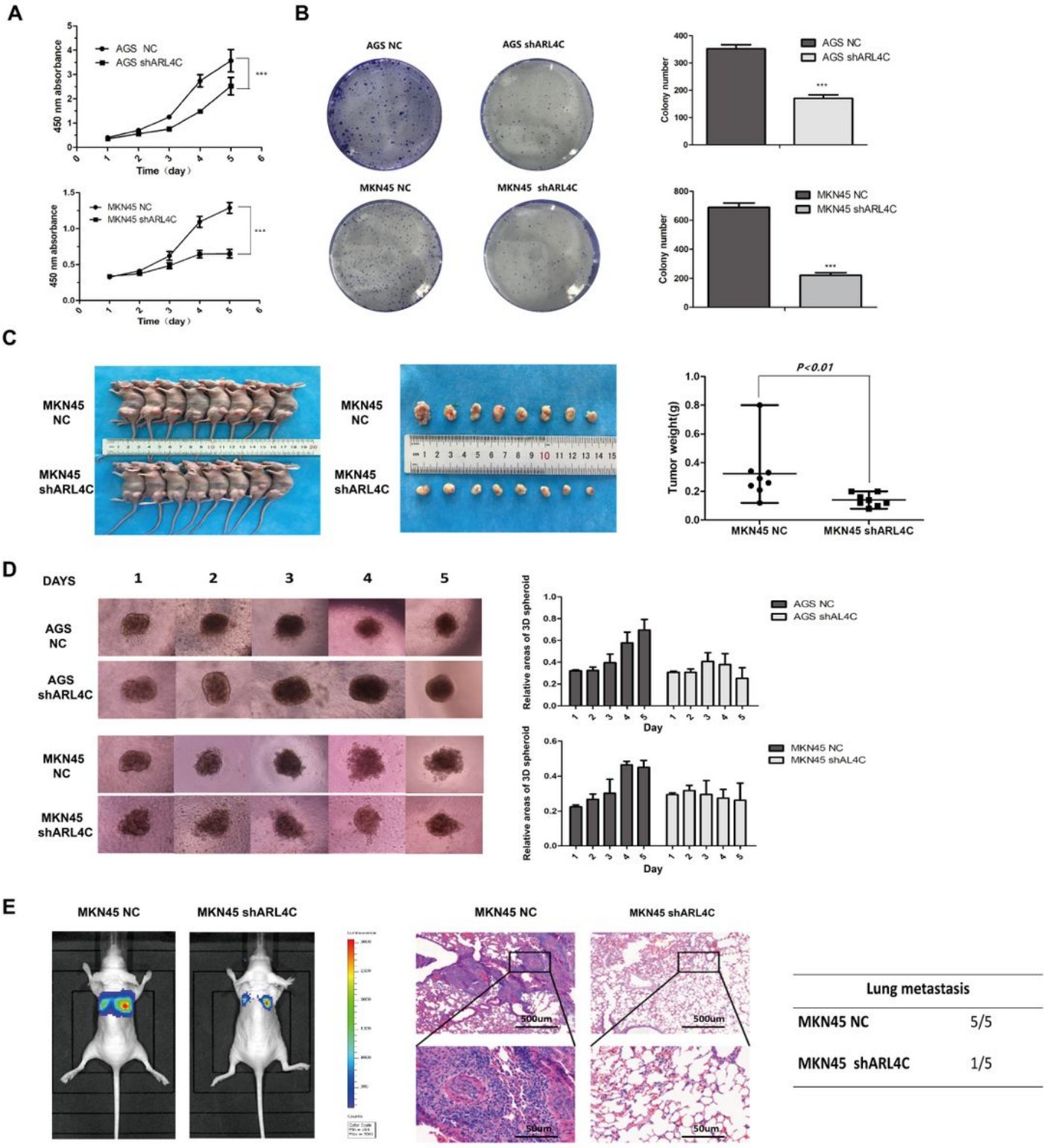

Lung metastasis	
MKN45 NC	5/5
MKN45 shARL4C	1/5

Figure 4

Silencing of ARL4C inhibits the proliferation and invasive capacities of GC cells. (a) Down-regulating ARL4C inhibits the cell viability of AGS and MKN45 cells. (b) Decreased ARL4C remarkably reduces the size and number of clones formed by AGS and MKN45 cells. (c) Representative images of tumors in nude mice (n=8) implanted with MKN45 cells expressing shARL4C or negative control (NC). The weights of the xenograft tumors are measured. (d) Down-regulating ARL4C inhibits the invasive ability of AGS and

MKN45 cells in 3D culture. (e) Representative bioluminescent imaging (BLI) of the different groups following tail vein injection (10 weeks). Representative H&E staining of lung tissues from the different groups. *P<0.05. The incidences of lung metastases in the different groups of nude mice.

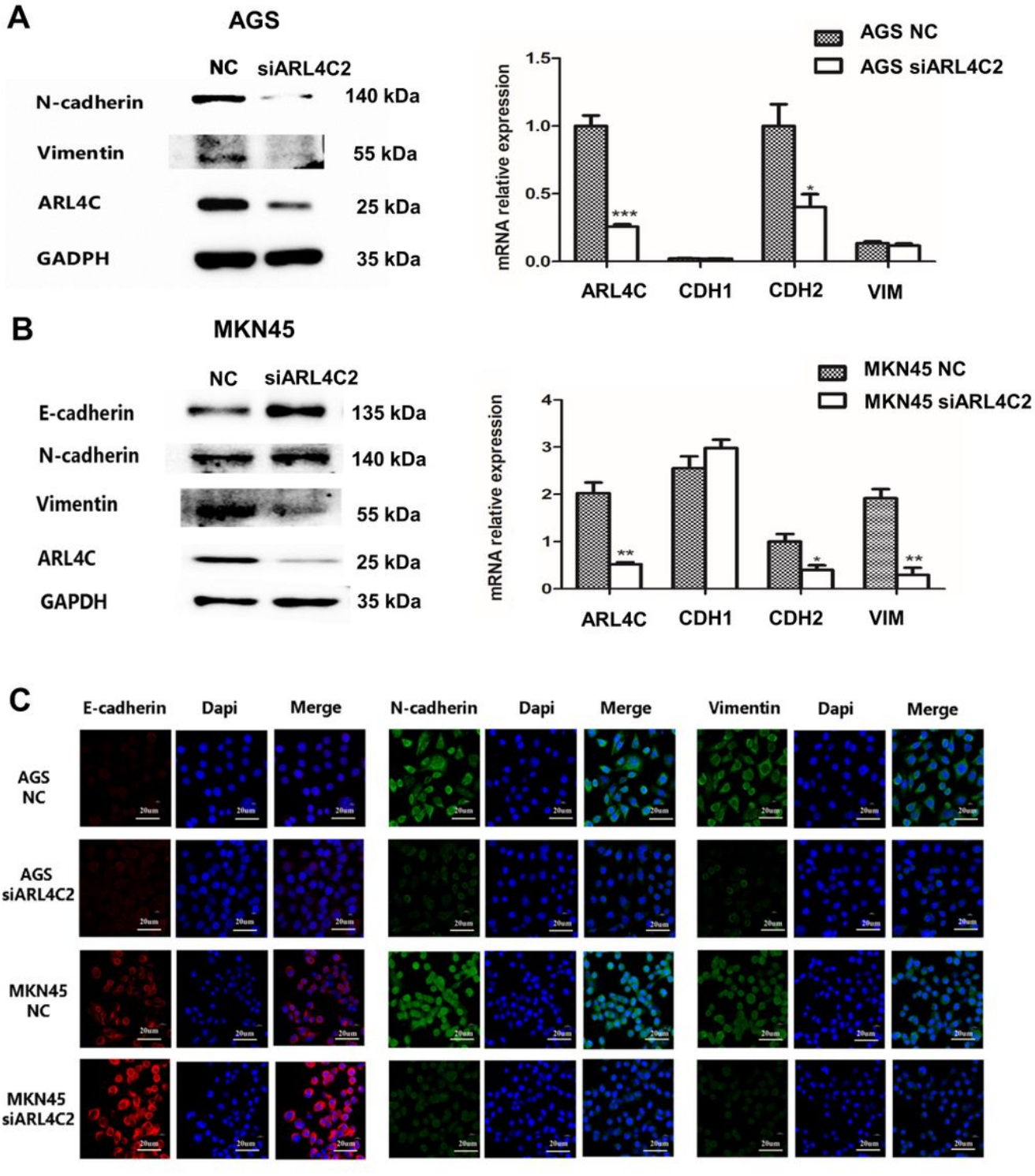

Figure 5

Silencing of ARL4C reverses EMT of GC cells. (a) Representative images of Western blot and RT-PCR show the changes of mesenchymal markers (N-cadherin and Vimentin) after ARL4C silencing in AGS

cells. (b) Representative images of Western blot and RT-PCR show the changes of epithelial marker (E-cadherin) and mesenchymal markers (N-cadherin and Vimentin) after ARL4C silencing in MKN45 cells. (c) After transfected with siARL4C2 or NC, AGS and MKN45 cells are fluorescence-stained for E-cadherin (red), N-cadherin (green), Vimentin (green) and DAPI (blue).

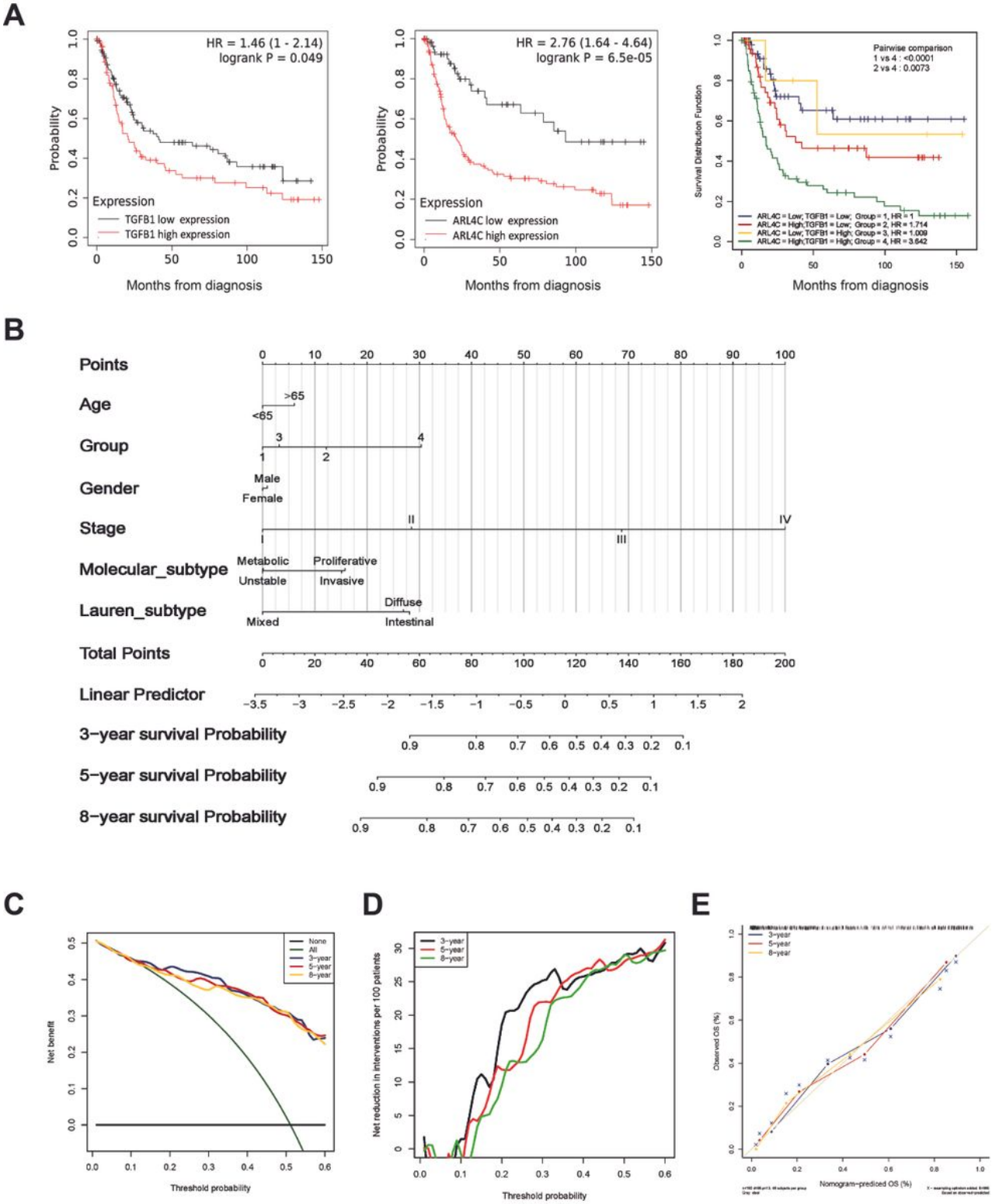

Figure 6

ARL4C enhances TGF-β1-mediated poor prognosis in GC. (a) Kaplan-Meier analysis of GC patient survival stratified according to TGF-β1 and ARL4C in GSE15459 cohort. (b) The OM nomogram based on multivariate analysis at 3, 5 or 8 years in GSE15459 cohort. (C and D) Decision curve analysis (DCA) for validating the predictive performance of the nomogram at 3, 5 or 8 years. (e) The calibration curves for the probability of survival show an optimal agreement of the prediction by the nomogram at 3, 5 or 8 years.

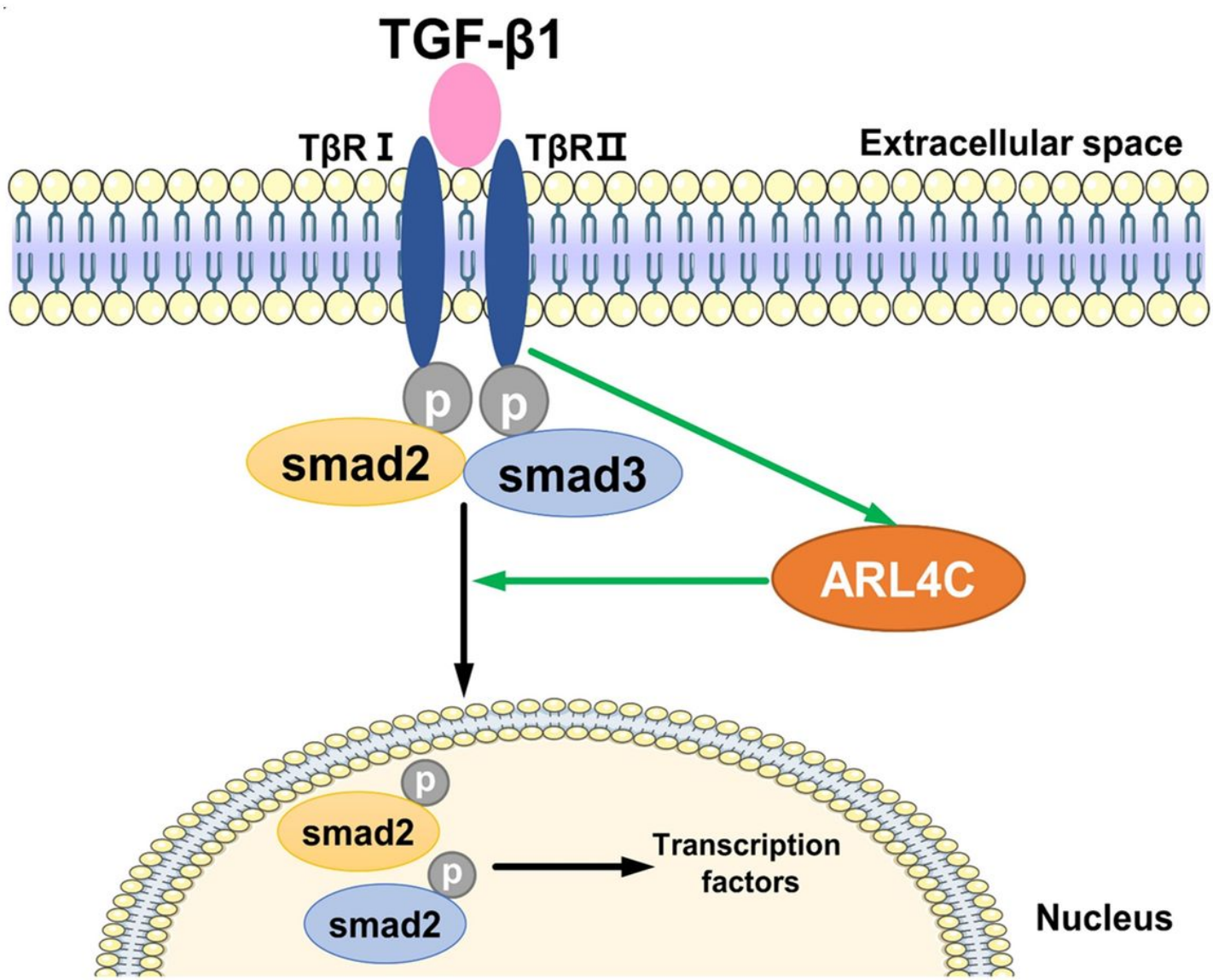

Figure 7

A schematic diagram shows that ARL4C functions as a mediator of TGF-β1/Smad signaling.

Supplementary Files

This is a list of supplementary files associated with this preprint. Click to download.

- supplement11.pdf